INFECTION AND IMMUNITY, Dec. 2006, p. 6599–6614 Vol. 74, No. 12
0019-9567/06/$08.00+0 doi:10.1128/IAI.01085-06

Helicobacter pylori VacA Toxin Promotes Bacterial Intracellular Survival in Gastric Epithelial Cells▽†

M. R. Terebiznik,[1,3] C. L. Vazquez,[2] K. Torbicki,[1,3] D. Banks,[1,3] T. Wang,[4] W. Hong,[4] S. R. Blanke,[5] M. I. Colombo,[2] and N. L. Jones[1,3]*

Infection, Injury, Immunity and Repair Program, Hospital for Sick Children, Toronto, Ontario, Canada[1]; IHEM-CONICET, Facultad de Ciencias Medicas, Universidad Nacional de Cuyo, Mendoza, Argentina[2]; Departments of Paediatrics and Physiology, University of Toronto, Toronto, Ontario, Canada[3]; Laboratory of Membrane Biology, Institute of Molecular and Cell Biology, Proteos, Singapore, Republic of Singapore[4]; and Department of Microbiology and Institute for Genomic Biology, University of Illinois, Urbana, Illinois[5]

Received 11 July 2006/Returned for modification 18 August 2006/Accepted 19 September 2006

Helicobacter pylori **colonizes the gastric epithelium of at least 50% of the world's human population, playing a causative role in the development of chronic gastritis, peptic ulcers, and gastric adenocarcinoma. Current evidence indicates that *H. pylori* can invade epithelial cells in the gastric mucosa. However, relatively little is known about the biology of *H. pylori* invasion and survival in host cells. Here, we analyze both the nature of and the mechanisms responsible for the formation of *H. pylori*'s intracellular niche. We show that in AGS cells infected with *H. pylori*, bacterium-containing vacuoles originate through the fusion of late endocytic organelles. This process is mediated by the VacA-dependent retention of the small GTPase Rab7. In addition, functional interactions between Rab7 and its downstream effector, Rab-interacting lysosomal protein (RILP), are necessary for the formation of the bacterial compartment since expression of mutant forms of RILP or Rab7 that fail to bind each other impaired the formation of this unique bacterial niche. Moreover, the VacA-mediated sequestration of active Rab7 disrupts the full maturation of vacuoles as assessed by the lack of both colocalization with cathepsin D and degradation of internalized cargo in the *H. pylori*-containing vacuole. Based on these findings, we propose that the VacA-dependent isolation of the *H. pylori*-containing vacuole from bactericidal components of the lysosomal pathway promotes bacterial survival and contributes to the persistence of infection.**

The gram-negative spirillum *Helicobacter pylori* efficiently infects human stomachs and colonizes the gastric mucosa in over half of the world's human population (41). Once established, *H. pylori* infection provokes a strong immune reaction, which instead of causing clearance of the pathogen, leads to a chronic inflammatory process that results in epithelial damage (31). Eventually, depending on specific host-pathogen interactions, a proportion of infected individuals will develop more severe sequelae, including peptic ulcer disease, gastric cancer, or mucosa-associated lymphoid tissue lymphoma (31).

Although generally considered an extracellular pathogen, expanding evidence indicates that *H. pylori* also invades gastric epithelial cells (34). One possible explanation for the persistence of *H. pylori* infection despite vigorous host immunological defenses and antibiotic therapy is the existence of an intracellular bacterial reservoir. *H. pylori* infection predominantly triggers a T helper type 1 immune response characteristic of intracellular pathogens (37). In addition, electron microscopy studies of gastric biopsy samples obtained from infected humans demonstrate the presence of *H. pylori* within epithelial cells (14, 54). Recently, intracellular bacteria were identified in gastric epithelial progenitor cells in a murine model of infection (27). Furthermore, the ability of *H. pylori* to invade mammalian epithelial cells has been documented in gastric adenocarcinoma-derived epithelial cell lines (3, 33, 35, 39). A study on bacterial entry demonstrated that *H. pylori* enters into gastric cells through a zipper-like phagocytic mechanism that requires protein kinase C and phosphatidylinositol 3-kinase (23). Amieva and colleagues (3) reported that following *H. pylori* invasion of AGS cells, large vacuolar compartments are formed in which the bacteria can persist for long periods. In addition, the authors demonstrated that *H. pylori* can egress from this compartment and infect other gastric cells. These observations could be of fundamental importance in understanding how the bacterium escapes from the host immune response and persists in the gastric epithelium. However, significant controversy still remains regarding the ability of the bacteria to invade epithelial cells and the bacterial factors involved. Furthermore, the mechanisms promoting intracellular survival of *H. pylori* remain uncharacterized.

The vacuolating toxin VacA is an important pathogenic factor for *H. pylori* (reviewed in reference 10). VacA contributes to bacterial colonization by unknown mechanisms. In addition, the presence of VacA impacts the development of peptic ulcer disease and gastric cancer. The *vacA* gene encodes a precursor protein which is processed to yield a secreted mature 88-kDa toxin (47). The mature toxin is organized into two domains, p33 and p55, which are required for activity of the toxin (26, 48, 52, 55). The most-well-studied effect of VacA intoxication of mammalian cells is the induction of vacuolation (10). The

* Corresponding author. Mailing address: Hospital for Sick Children, 555 University Ave., Toronto, Canada M5G 1X9. Phone: 416-813 7062. Fax: 416-813 6531. E-mail: nicola.jones@ sickkids.ca.

† Supplemental material for this article may be found at http://iai.asm.org/.

▽ Published ahead of print on 25 September 2006.

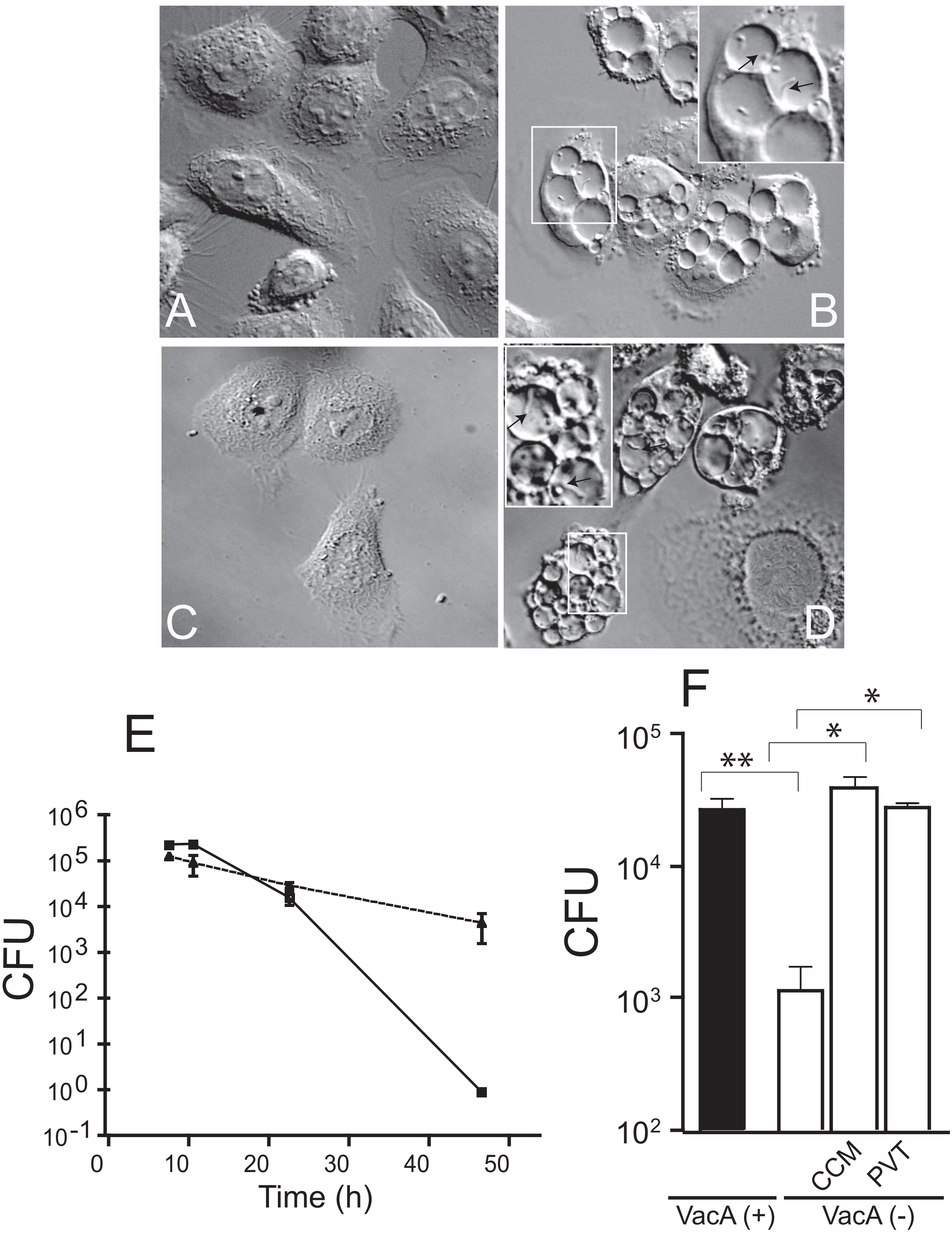

A
B
C
D
E
F
CFU
10^{6}
10^{5}
10^{4}
10^{3}
10^{2}
10^{1}
10^{0}
10^{-1}
0
10
20
30
40
50
Time (h)
**
*
*
CCM
PVT
VacA (+)
VacA (-)

vacuolation of late endosomal compartments is thought to be mediated by several factors, including the vacuolar ATPase (12), the small GTPase Rab7 (10, 24), dynamin (44), and syntaxin 7 (43). In addition to vacuolation, VacA has pleiotropic effects on mammalian cells, including induction of apoptosis (11, 16, 51), inhibition of T-cell proliferation (4, 17, 42), altered antigen processing (25), and disruption in permeability of monolayers (29). We and others have also shown that VacA plays a fundamental role in arresting phagosome maturation following *H. pylori* infection of macrophages (10, 15, 57). However, the role of this toxin in the formation of the bacterial intracellular niche and bacterial survival inside gastric epithelial cells remains unclear (3, 15, 34, 35). Thus, we characterized the role of VacA in establishing *H. pylori*'s compartment within gastric epithelial cells.

MATERIALS AND METHODS

Reagents and antibodies. Ham's F-12, Dulbecco's modified Eagle's medium, and fetal calf serum were from Wisent (St. Bruno, Quebec, Canada). FuGENE-6 was purchased from Roche Diagnostics (Indianapolis, IN). Fluorescein isothiocyanate (FITC)-, Cy5-, and Cy3-conjugated antibodies were from Jackson ImmunoResearch Laboratories (West Grove, PA). Mouse monoclonal anti-LAMP-1 antibodies were from the Developmental Studies Hybridoma Bank (Iowa City, IA). Rabbit anti-*H. pylori* antibodies were from DAKO (Denmark). Anti-c-Myc antibody was from Santa Cruz Biotechnology (Santa Cruz, CA). Cathepsin D antibodies were from Upstate Biotechnology (Lake Placid, NY). FM4-64, DQ red-bovine serum albumin (BSA), and the fluorescent probes utilized for labeling of the intracellular compartment were from Molecular Probes (Eugene, OR). All other reagents were obtained from Sigma-Aldrich (St. Louis, MO). Latex beads were supplied by Bangs Laboratories, Inc. (Fishers, IN).

Cells and bacterial growth conditions. Culture conditions for human gastric epithelial cells (AGS) (3) and Chinese hamster ovary cells stably transfected with FcγIIa receptors (CHO-IIa) (49) have been previously described. Growing conditions for wild-type *H. pylori* strain 60190 (ATCC 49503; *cagA*$^+$ *cagE*$^+$ VacA$^+$) and its isogenic *vacA* mutant strain (kindly provided by Richard Peek, Jr., Nashville, TN) were as described previously (57).

Plasmid and transfection reagents. The generation of plasmids used for expression of RILP and RILP-C33 (8) and green fluorescent protein (GFP)-conjugated Rab7 and Rab5 (49), GFP-conjugated Rab34 and Rab7 mutants F45A and V180A (53) and myc-tagged RILP mutant I251A (53), GFP-CD63 (2), myc-tagged FcγIIa receptor (FcIIa) (13), and GFP-PX (22) have all been described previously. The RILP-C33 plasmid was a kind gift from Cecilia Bucci (Lecce, Italy). In all cases, the cells were transiently transfected using FuGENE-6 (Roche Molecular Biochemicals) as suggested by the manufacturer.

Cell invasion and intoxication assays. *H. pylori* strains were grown at 37°C in brucella broth (Difco Laboratories, Detroit, Mich.) supplemented with 10% heat-inactivated fetal bovine serum (Gibco BRL Life Technologies, Gaithersburg, Md.) under microareophilic conditions. After overnight incubation, the bacteria were pelleted and resuspended to an optical density of 0.4 to 0.5 (620 nm) in cell culture media. Cell invasion was performed on 70 to 80% confluent cell cultures in six-well culture plates. After a 3-h incubation, unattached bacteria were removed by washing the cells four times with phosphate-buffered saline (PBS) and cell-adherent *H. pylori* cells were allowed to internalize for an additional 4 h. In order to prevent any extracellular bacterial growth, the culture medium was supplemented with gentamicin (100 μg/ml). After 12 h of invasion, the amount of gentamicin in the medium was reduced to 10 to 20 μg/ml. Intracellular bacteria were retrieved from invaded cells utilizing 1% saponin in PBS buffer, as described previously (3). Serial dilutions of bacterial suspensions were plated in brucella agar supplemented with 10% fetal calf serum and incubated for 96 h in microaerophilic conditions for CFU determinations.

Phagocytosis of latex beads (3 μm) by CHOIIa cells and FcIIa transiently transfected AGS cells was performed as described elsewhere (49). After phagocytosis, cells were incubated with *H. pylori* for a 4-h period and treated with gentamicin (100 μg/ml) overnight. Extracellular latex beads were detected by immunolabeling with FITC-conjugated goat anti-human immunoglobulin G (IgG) or FM 4-64 labeling. Expression of myc-tagged FcIIa receptor in AGS cells was monitored by immunolabeling with anti-myc antiserum (data not shown).

For cell intoxication with VacA toxin, wild-type *H. pylori* culture supernatants (optical density [OD] = 1.0 at 620 nm) were filtered through a 0.22-μm-cutoff membrane filter and concentrated 10 times using a 50-kDa-cutoff Amicon Ultra centrifugal filter (Millipore). In experiments, concentrated culture medium (CCM) was utilized at 1.5 times final concentration.

VacA toxin was purified from *H. pylori* 60190 (ATCC 49503; *cagA*$^+$ *cagE*$^+$ s1m1 VacA$^+$) culture supernatants utilizing ammonium sulfate (50%) precipitation and fast protein liquid chromatography as was previously described by Patel et al. (30). Purified VacA toxin (PVT) was activated by incubation in acidified Ham's F-12 culture medium, pH 2, for 30 min at 37°C. For cell intoxication, 10^6 AGS cells were incubated in the presence of activated purified VacA toxin (26.5×10^{-3} μM) for the time periods indicated in each experiment (30).

The unpaired *t* test and other statistical analyses of the results were performed utilizing GraphPad Prism 4 for Macintosh V 4.0b.

Immunofluorescence and confocal microscopy. Prior to immunostaining, cells were fixed for 20 min in 4% formaldehyde in PBS, permeabilized by incubation in 0.1% (vol/vol) Triton X-100 in PBS for 20 min, and blocked for 30 min with 5% milk in PBS (vol/vol). All steps were carried out at room temperature.

For immunofluorescence, permeabilized cells were incubated with primary antibody for 1 h at room temperature, washed extensively, and then incubated with secondary antibodies for 1 h at room temperature. The following primary antibodies were used at the indicated dilutions: cathepsin D, 1:100; LAMP-1, 1:1,000; Myc, 1:200; and *H. pylori*, 1:20.

Fluorescence microscopy, photobleaching, and image analysis. Fluorescence and differential interference contrast (DIC) micrographs were obtained using a fluorescent Leica DM-IRE2 microscope. Confocal image acquisition was performed using either a Zeiss LSM 510 microscope or a spinning disc system consisting of a Leica DM-IRE2 microscope equipped with a Visitech Int. QLC100 microlens head, a Hamamatsu Orca AG Deep cooled digital camera, a Melles Griot argon ion laser 643 system, and the appropriate set of excitation and emission filters placed in wheels driven by a Ludt controller. Openlab (Improvision) was used for image acquisition. Images were acquired with a ×100 oil immersion objective. A heated microscope stage was used to maintain the temperature at 37°C during image acquisition when using live cells. For quantitation, images were imported into Image J (http://rsb.info.ni*H*.gov/ij/), and the mean fluorescence per pixel was measured using the measurement tool. Quantification of the degree of colocalization between two markers was performed using the colocalization module of Openlab 4.0.1 on defined regions of interest.

Fluorescence recovery after photobleaching (FRAP) was estimated as previ-

FIG. 1. VacA toxin is involved in the formation of the *H. pylori* intracellular niche and promotes bacterial survival. A DIC micrograph of uninfected control AGS cells is shown in panel A. AGS cells after 24 h of invasion with wild-type *H. pylori* is shown in panel B. The inset in panel B shows details of the *H. pylori*-containing vacuoles. Arrows point to intracellular bacteria inside the vacuolar compartment. Panel C shows AGS cells after 24 h of invasion with *H. pylori vacA* mutant strain. After 10 h of infection with the *H. pylori vacA* mutant strain, AGS cells were treated with wild-type *H. pylori* conditioned culture medium for 24 h (D). The inset in panel D shows details of the *H. pylori*-containing vacuoles, and the arrows point to intracellular bacteria inside the vacuolar compartment. AGS cells were infected with wild-type or *vacA* mutant *H. pylori* strains under gentamicin assay conditions (see Materials and Methods). At the indicated invasion times, intracellular *H. pylori* cells were retrieved from AGS cells utilizing 1% saponin in PBS buffer and plated on brucella agar. Intracellular survival (CFU) of wild-type (triangles) and *vacA* mutant (squares) *H. pylori* strains is shown in panel E. (CFU values corresponded to means ± standard error from a single representative experiment performed in triplicate. These results were reproduced on four separate occasions). AGS cells were infected with wild-type [VacA (+)] or VacA-negative mutant [VacA (−)] *H. pylori*. Three hours after infection with the *vacA* mutant strains, AGS cells were treated with wild-type *H. pylori* CCM or PVT, and intracellular survival (CFU) of the bacteria was determined using the gentamicin protection assay at the 36-h invasion time point (F). (CFU values corresponded to means ± standard error from a single representative experiment performed in triplicate. These results were reproduced on four separate occasions.) *, $P = 0.0001$; **, $P = 0.0003$.

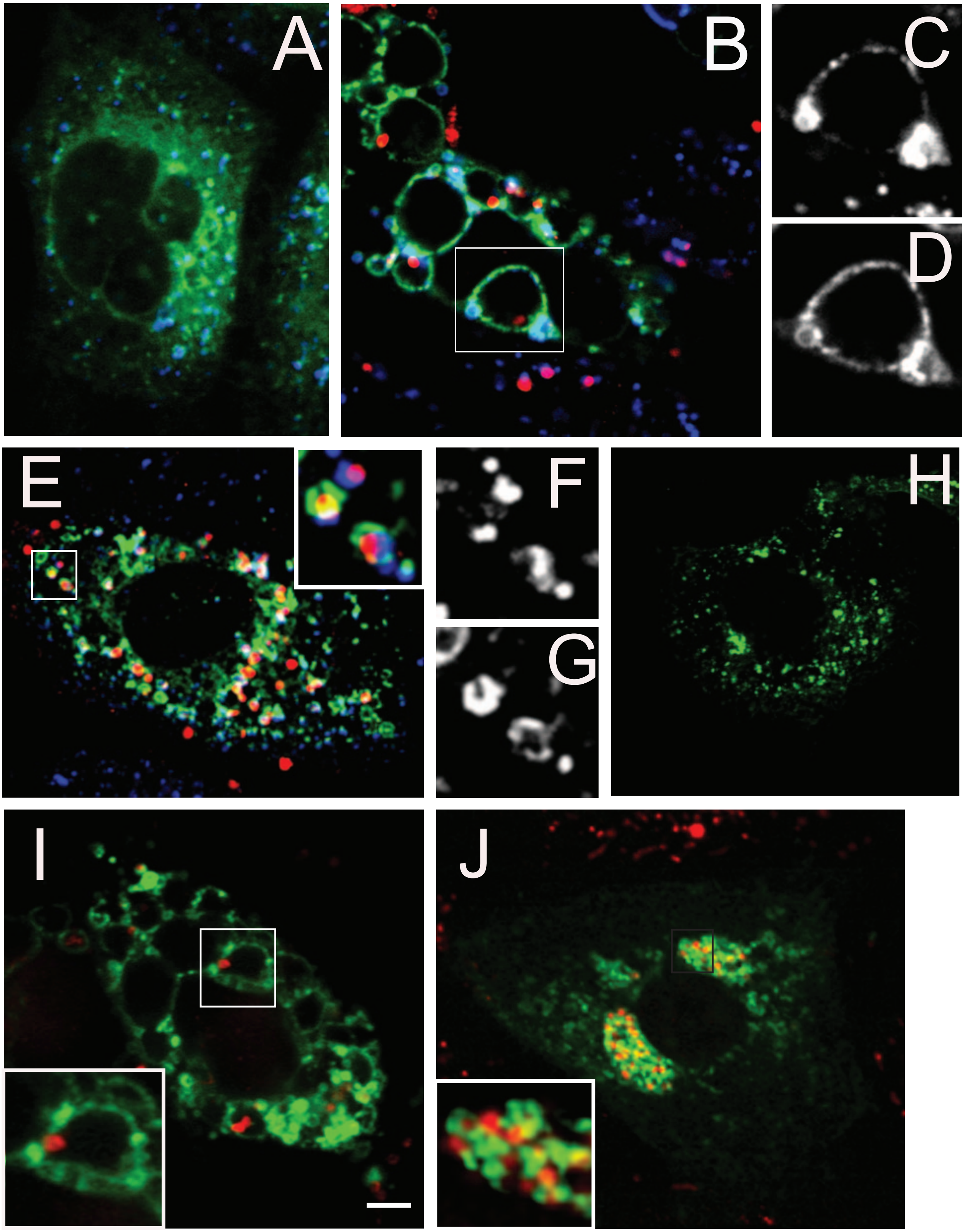

FIG. 2. *Helicobacter pylori*'s intracellular compartment acquires late endosomal and lysosomal markers. Panels A and B show the distribution of GFP-Rab7 (green) and Lamp-1 (blue) protein for control (A) and wild-type *H. pylori*-invaded cells (B). Details of the vacuolar compartment showing Lamp1 and Rab7 recruitment are presented in panels C and D, respectively. Panel E shows the distribution of GFP-Rab7 (green) and Lamp-1 (blue) for AGS cells invaded by an *H. pylori vacA* mutant strain. The inset in panel E shows in detail the morphology of the intracellular compartment of the *vacA* mutant bacteria. The recruitment of Lamp1 and Rab7 to the bacterial compartment is shown in detail in panels F and G, respectively. Panels H to J show the distribution of GFP-CD63 (green) for uninfected AGS cells (H) and AGS cells infected with wild-type (I) or VacA mutant (J) *H. pylori*, respectively. The insets in panels I and J show details of the bacterial niches. All of the microphotographs were taken with a spinning disk confocal microscope with a ×100 oil objective. The scale bar in panel I is equivalent to 3 μm. Immunolabeled bacteria are shown in red. For all experiments, the invasion time was 24 h.

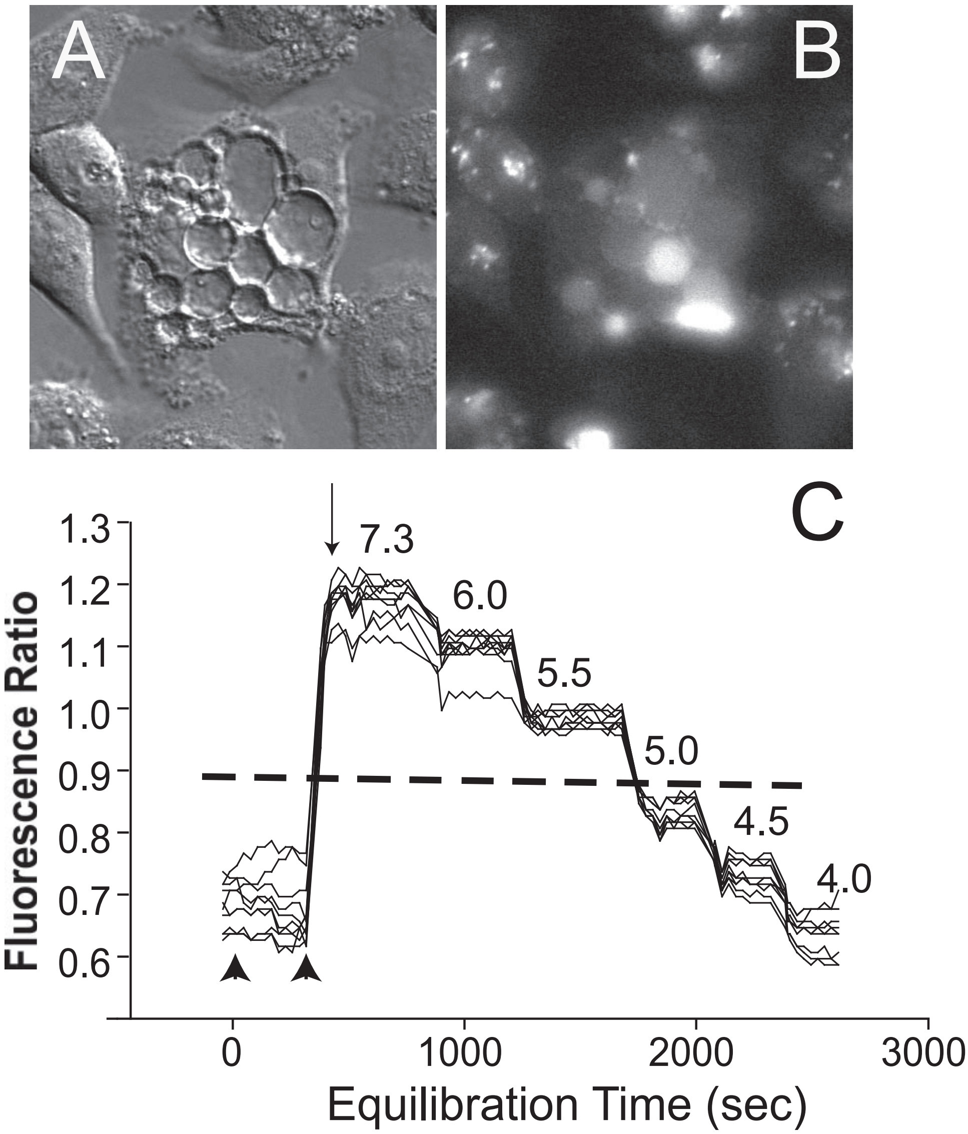

FIG. 3. Assessing the pH of *H. pylori*'s intracellular compartment. *H. pylori*-containing vacuoles loaded with the pH-sensitive fluorescent dye Oregon green 514 are shown in panels A (DIC of invaded cells) and B. The result of a typical pH determination assay representative of three independent experiments is shown in panel C. Oregon green fluorescent ratio (excitation at 510/450 nm detected at 530) were measured in 10 different bacterial compartments distributed in different cells along the microscope optical field (black lines) and plotted as a function of the pH equilibration time. An average of the ratio for the fluorescent background of the field was obtained in a cell-free area (dashed line). The section of the curve between two arrowheads indicates the fluorescent ratio for *H. pylori* vacuoles at the resting state in isosmotic Na solution. The arrow indicates the time when nigericin isosmotic K^+ solution was added and the onset for the pH calibration of the bacterial compartments. The pH corresponding to each equilibration time is indicated above the curves. The fluorescence ratio/pH titration curve is shown in figures in the supplemental material.

ously described by Vieira et al. (49). Briefly, AGS cells were transfected with GFP-Rab7 and invaded with *H. pylori* as described above. *H. pylori*-containing vacuoles were photobleached using the 488-nm laser line of the Zeiss LSM 510 confocal microscope at full power. The recovery of fluorescence was then monitored over time by scanning the bleached area, minimizing photobleaching during sampling. To analyze the rate of recovery, we compared the fluorescence of the bleached area to that of an adjacent unbleached area of the same cell with a similar fluorescence intensity. For each time point, the fluorescence of the bleached area was normalized to that of the corresponding control (unbleached) area. Nonlinear regression fitting of FRAP data was performed utilizing Graph Pad Prism 4 software.

Ratiometric fluorescence microscopy. For the measurement of lysosomal and vacuolar pH, AGS cells were incubated in the presence of 1 mg/ml of Oregon green-dextran, M_r 10,000, for 2 h before and 2 h after the onset of invasion. After this, cells were washed and incubated overnight utilizing the conditions for invasion indicated above. Ratiometric measurements were performed as previously indicated (6). Briefly, resting pH values were obtained in cells bathed in sodium-rich medium (140 mM NaCl, 5 mM glucose, 15 mM HEPES, pH 7.4) at 37°C. Calibration of fluorescence versus pH was obtained by replacing the sodium-rich buffer with potassium-rich medium (140 mM KCl, 5 mM glucose, 15 mM HEPES), adjusted to the desired pH with KOH, followed by addition of nigericin (5 μM). The microscope and software setup used for ratio imaging have been described in detail elsewhere (6).

RESULTS

VacA contributes to the formation of the bacterial niche in AGS cells. In order to characterize *H. pylori's* intracellular niche, AGS cells were infected with *H. pylori* and monitored

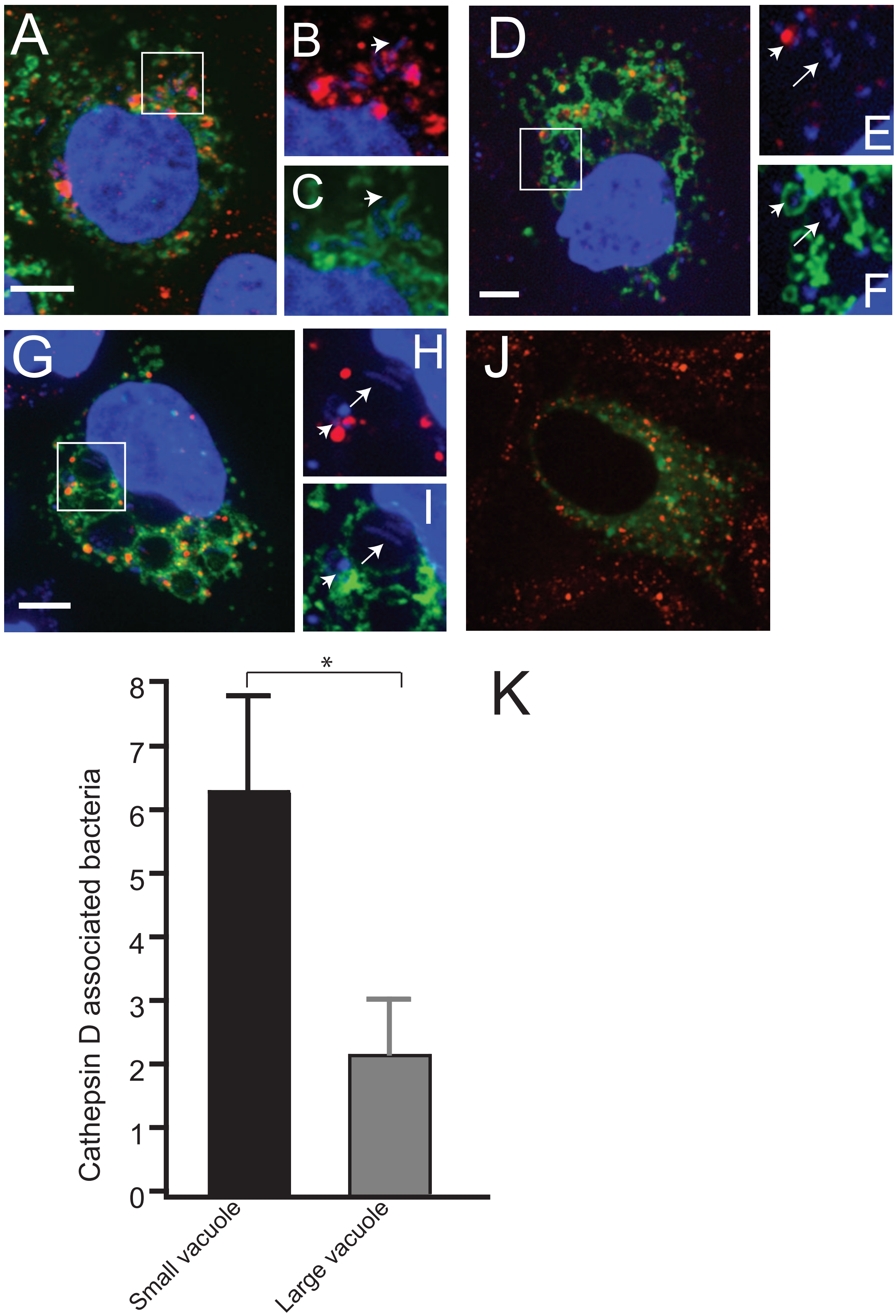
A
B
C
D
E
F
G
H
I
J
K
*
Cathepsin D associated bacteria
0
1
2
3
4
5
6
7
8
Small vacuole
Large vacuole

for 48 h postinfection. As previously reported by Amieva et al. (3), 6 h after infection, viable and highly motile spiral *H. pylori* cells were detected inside large vacuoles by DIC live microscopy. A representative DIC micrograph of AGS cells after 24 h of infection with *H. pylori* is shown in Fig. 1A and B (see movie S1 in the supplemental material, which demonstrates viable motile bacteria within the majority of the vacuoles). Previous studies indicate that VacA enhances bacterial survival in professional phagocytic cells, but the role of the toxin during invasion of gastric cells is controversial (15, 34, 57). Furthermore, the contribution of VacA to the formation of the large intracellular niche has not been evaluated yet. Therefore, we utilized an isogenic *vacA* mutant strain to define the role of VacA. Infection of AGS cells with *vacA* mutant *H. pylori* did not produce any discernible vacuolar compartment as assessed by DIC microscopy (Fig. 1C). However, fluorescence immunolabeling of infected cells utilizing *H. pylori* antibodies demonstrated that the *vacA* mutant strain maintained the ability to invade AGS cells (see Fig. S1A and B in the supplemental material). When host cells infected with *vacA* mutant strain were subsequently incubated with PVT or CCM obtained from wild-type but not *vacA* mutant *H. pylori*, motile *vacA* mutant *H. pylori* cells were found in large intracellular compartments (Fig. 1D and see movie S2 in the supplemental material). Taken together, these results indicate that the generation of the large *H. pylori* compartment, but not the capacity to invade AGS cells, was dependent on the vacuolating cytotoxin.

Next, we determined the effect of VacA toxin on the intracellular survival of *H. pylori*. AGS cells were infected with wild-type or *vacA* mutant *H. pylori* and subsequently incubated with the cell-impermeant antibiotic gentamicin to kill extracellular bacteria. At less than 24 h of infection, both the wild-type and *vacA* mutant bacteria displayed similar levels of intracellular survival. However, wild-type *H. pylori* displayed enhanced intracellular survival compared with the isogenic *vacA* mutant at both 36 and 48 h (Fig. 1E and F). Importantly, the intracellular survival of the *vacA* mutant strain could be restored to the level of wild-type bacteria by incubating invaded cells with either purified VacA toxin or CCM from VacA-positive *H. pylori* (Fig. 1F). In support of these findings, a previous report by Petersen et al. (35) demonstrated that 24 h after the infection of AGS cells, the intracellular survival of two different strains of *H. pylori* depended on their ability to produce VacA toxin. Furthermore, we determined that the incubation of CCM from wild-type bacteria with cells infected with *vacA* mutant *H. pylori* resulted in an alteration of the intracellular compartment of the mutant bacteria as assessed by live-cell imaging (see movie S2 in the supplemental material). Taken together, these results suggest that *H. pylori* intracellular survival is a process that depends on several factors. However, VacA preferentially improves long-term intracellular survival of *H. pylori*, likely by securing a specific intracellular niche for the bacteria.

***H. pylori*-containing vacuoles are derived from late endocytic compartments.** To generate an intracellular niche, invasive bacterial species subvert host cell membrane trafficking pathways through the action of protein effectors. These effectors promote the progressive and coordinated fusion of the pathogen-containing vacuole with specific host cell compartments, thereby avoiding intracellular antimicrobial defenses (1, 7). To further characterize the *H. pylori*-containing vacuole, we investigated the presence of well-established markers for the cellular endocytic pathway by using confocal microscopy.

After 24 h of infection, markers of the early endocytic pathway including the membrane lipid phosphoinositide 3-phosphate and the small GTPase Rab5 were not detected on *H. pylori*-containing vacuoles (see Fig. S2A to D in the supplemental material). However, at this time point, the late endocytic marker Rab7 was present on both the large vacuoles containing wild-type *H. pylori* and the small vacuoles that tightly enclosed *vacA* mutant bacteria (Fig. 2A to H). The late endosomal markers, Lamp1 (Fig. 2A to H) and Limp1 (CD63) (Fig. 2I and J) were also recruited to *H. pylori*-containing vacuoles in a similar distribution to Rab7. Thus, the intracellular niche generated by both *vacA* mutant and wild-type *H. pylori* displayed characteristics of late endocytic compartments.

Late endosomes interact and fuse with lysosomes, which are rich in hydrolytic enzymes and antimicrobial agents. The finding that *H. pylori* survives within these late endosome-like compartments suggests that the bacterium actively avoids fusion with lysosomes and/or deactivates the microbicidal components of this organelle. Since an acidic pH is required for the proper functioning of these organelles, we next determined if the survival advantage observed for VacA-positive *H. pylori* was related to a higher pH in the vacuolar environment. Previous studies (3) using the acidotrophic dye LysoSensor indicated that the *H. pylori*-containing vacuole was slightly acidic. In order to precisely measure this parameter, we utilized the pH-sensitive fluorescent probe Oregon green 514-dextran (pK_a = 4.7) in a ratiometric fluorescence microscopy assay.

FIG. 4. VacA toxin prevents the sorting of cathepsin D to *H. pylori*-containing vacuoles in invaded AGS cells. Panel A shows GFP-Rab7 (green)-transfected AGS cells invaded with VacA mutant *H. pylori* bacteria. Thirty-two hours after infection, cells were fixed, permeabilized, and immunolabeled for cathepsin D (red). *H. pylori* cells were labeled with DAPI (4′,6′-diamidino-2-phenylindole) (blue). Panels B and C show in detail the bacterial intracellular niche from the area enclosed in panel A**.** Panel D shows GFP-Rab7 (green)-transfected AGS cells invaded with wild-type *H. pylori*. Cells were fixed, permeabilized, and immunolabeled for cathepsin D (red). *H. pylori* was labeled with DAPI (blue). Panels E and F show in detail the bacterial intracellular niche from the area enclosed in panel D**.** Ten hours after infection with *vacA* mutant *H. pylori*, GFP-Rab7-expressing AGS cells (green) were incubated for 20 h with wild-type conditioned growth medium (CCM) (G). Cells were fixed, permeabilized, and immunolabeled for cathepsin D (red). *H. pylori* was labeled with DAPI (blue). An uninfected AGS cell expressing GFP-Rab7 (green) and immunolabeled for cathepsin D (red) is shown in panel J**.** The average number of cathepsin D-positive bacteria in either large or small compartments per cell is shown in panel K. Intracellular wild-type *H. pylori* cells were scored according to their association with cathepsin D and the size of the vacuolar compartment. Small compartments were arbitrarily defined as vacuoles that closely surround the bacteria (arrowheads), while large compartments clearly surpassed the bacterial volume (arrows). The number of bacteria was assessed from 15 infected cells utilizing z-stack micrograph slices obtained each 0.25 μm by confocal microscopy. *, P = 0.03. The white bars in the micrographs indicate 10-μm scale. Original magnification, ×1,000.

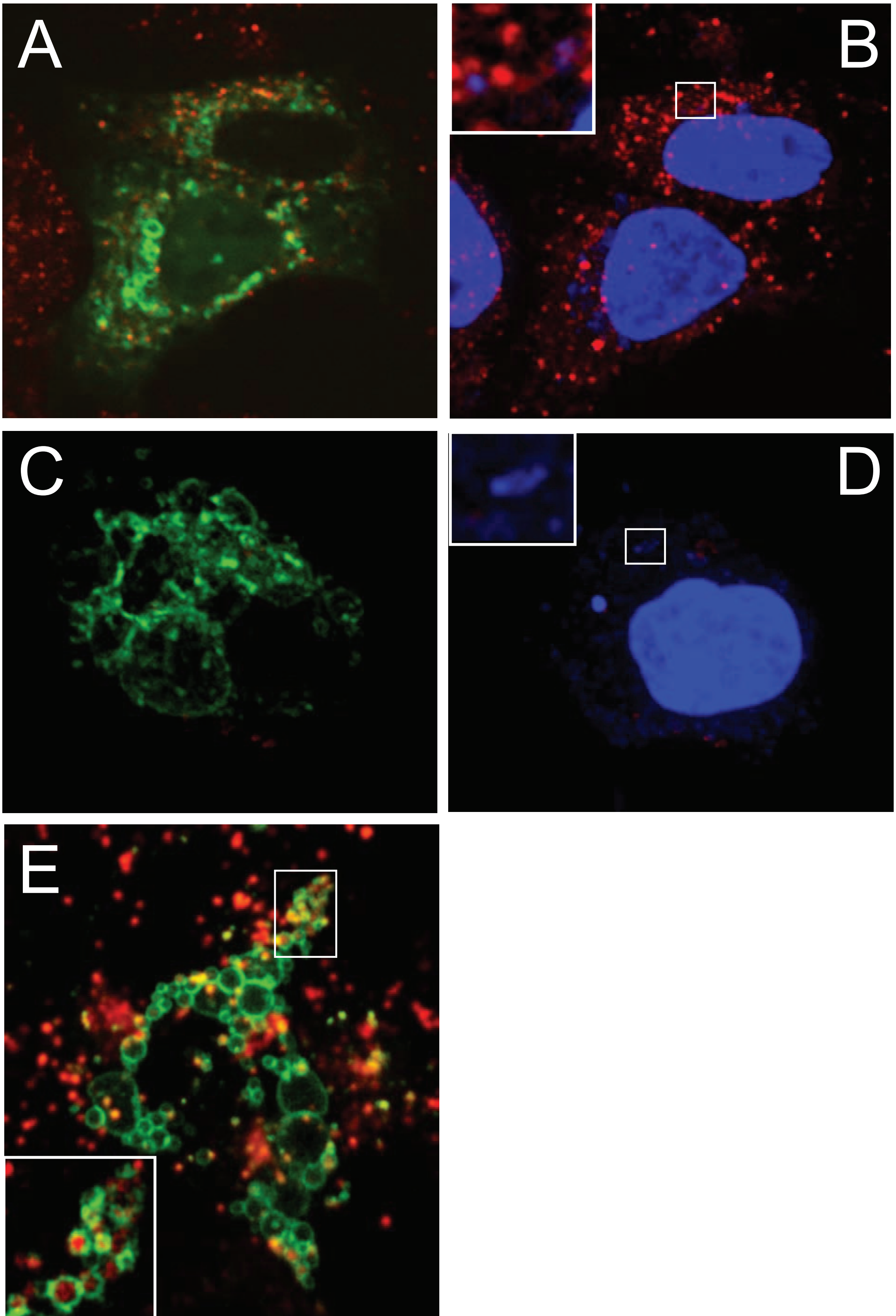
A
B
C
D
E

The dye was loaded by endocytosis into AGS cells before *H. pylori* infection and subsequently chased for 2 h to allow accumulation in late endocytic compartments. Following *H. pylori* infection, the fluorescent probe was detected in the bacterium-containing compartments, indicating that the bacterial vacuole merged with late endocytic organelles (Fig. 3A and B). In agreement with previous reports (6, 13, 32), we measured a pH of 4.97 ± 0.15 for lysosomal organelles in control cells (data not shown). In three independent experiments, 71% of the vacuoles showed a pH that fell below the lower level of detection of the assay, a pH of 4 (Fig. 3C; also see the titration curve in Fig. S3 in the supplemental material). By considering the remaining values obtained within the level of detection of the assay, we estimated the pH of the bacterium-containing compartment was 4.38 ± 0.07. These results indicate that VacA-mediated enhanced survival of intracellular *H. pylori* was not due to elevated vacuolar pH.

We next examined the presence of the lysosomal protease cathepsin D during infection. Cathepsin D was clearly present in the tight compartments containing *vacA* mutant bacteria (Fig. 4A to C). In contrast, there was significantly less cathepsin D colocalization with intracellular wild-type bacteria in large vacuoles (Fig. 4D to F and K). Similarly, when *vacA* mutant bacterium-infected cells were incubated with wild-type concentrated supernatants, there was significantly less cathepsin D colocalization at the large intracellular niche containing *vacA* mutant bacteria (Fig. 4G to I). Under these conditions, the protease was mainly associated with the smaller vacuoles containing bacteria (Fig. 4D to I). These results suggest that VacA-positive bacteria generate a compartment in which exposure to degradative lysosomal components such as cathepsin D may be reduced. In support of these findings, we evaluated the capacity of infected cells to degrade a chromogenic substrate (DQ-BSA) loaded by endocytosis. As in shown in Fig. 5, cells infected with the *vacA* mutant strain efficiently hydrolyzed the substrate, resulting in detection of the fluorescence signal both in bacterium-containing compartments and lysosomes (see inset in Fig. 5B). In marked contrast, although wild-type *H. pylori*-infected cells maintained the ability to take up fluid-phase markers (Fig. 5E), minimal to no fluorescence of DQ-BSA was detected in these vacuolated cells, indicating that lysosomal degradation was not occurring (Fig. 5C and D). Taken together, these results suggest that while *vacA* mutant *H. pylori* cells can survive within their intracellular compartment for a limited period of time, the presence of VacA enhances survival of *H. pylori* in a manner that correlates with development of an intracellular late endosomal/lysosomal niche deficient in degradative microbicidal activities.

VacA-mediated fusion of late endosomal-lysosomal compartments promotes formation of *H. pylori*'s large intracellular niche. We next investigated the morphogenesis of *H. pylori*'s intracellular niche. The current proposed mechanism for VacA-mediated vacuolation suggests that VacA creates an anion-selective pore in acidic organelles (10, 46). As a consequence, osmotically active species accumulate, particularly protonated weak bases, prompting swelling of these compartments and cell vacuolation. However, several lines of evidence suggest that endosomal homotypic fusion events could also be involved (15). Due to the considerable size of *H. pylori*-containing vacuoles (up to 20 μm in diameter, or more), we hypothesized that swelling alone would not be sufficient and that fusion events could also be involved. To investigate this possibility, we designed an experiment taking advantage of the properties of CHO cells expressing IgG FcIIa receptors (CHOIIa), which are a valid working model to study membrane trafficking and maturation of phagosomes (49). These cells phagocytose IgG-opsonized latex beads, generating phagosomes, which subsequently mature into late endosomal compartments termed engineered phagolysosomes (49). Opsonized 3-μm latex beads were utilized to monitor the fate of late endosomal organelles in CHOIIa cells during infection with *H. pylori*. Following uptake of latex beads, phagolysosomes in uninfected CHOIIa cells contain a single bead. In marked contrast, 2 h after the phagocytosis of latex beads, subsequent *H. pylori* infection resulted in the formation of large Rab7-labeled phagolysosomes clearly loaded with multiple beads indicative of compartment fusion (Fig. 6A and B). The fusion event occurred only in the presence of wild-type bacteria, but failed to occur when cells were infected with the isogenic *vacA* mutant strain (Fig. 6C). We next validated this result in human gastric cells. Like CHOIIa cells, AGS cells expressing FcIIa receptor were able to internalize opsonized latex beads and formed engineered phagosomes labeled with GFP-Rab7 (Fig. 7A and B). Each latex bead internalized by AGS cells developed into a phagosome that contained a unique single bead (Fig. 7B). Following the phagocytosis of latex beads, infection of AGS cells expressing FcIIa receptor with VacA-positive *H. pylori* produced large Rab7-labeled vacuoles loaded with multiple beads (Fig. 7C and D). Live-cell imaging of wild-type *H. pylori*-infected AGS cells demonstrated that viable motile bacteria and latex beads coexisted in these large vacuoles (Fig. 7G and H and see movie S3 in the supplemental material). This phenotype was completely dependent on the VacA toxin, since engineered phagolysosomes in cells exposed to *vacA* mutant *H. pylori* were undistinguishable from those observed in uninfected cells (Fig. 7E and F). Thus, VacA can promote the homotypic fusion of late endosomal compartments, including individual bacterium-containing vacuoles, resulting in the formation of a unique intracellular niche for *H. pylori*.

The role of the Rab7-RILP complex in the morphogenesis of the *H. pylori*-containing vacuole. We next investigated the mechanisms responsible for the morphogenesis of the VacA-mediated bacterial niche. The small GTPase Rab7 is a key component of the membrane trafficking machinery involved in

FIG. 5. *H. pylori* invasion of AGS cells inhibits lysosomal protease activity in a VacA-dependent manner. GFP-Rab7 (green)-expressing cells were infected with *vacA* mutant bacteria (A and B) or wild-type (C and D) *H. pylori*. Following 24 h of infection, the cells were incubated with the chromogenic protease substrate DQ red-BSA (red) for a 3- to 4-h period. After this time, the cells were fixed and the bacteria were labeled with DAPI (4′,6′-diamidino-2-phenylindole). Panel E shows GFP-Rab7 (green)-expressing cells infected with wild-type *H. pylori*. Twenty-four hours later, the cells were incubated with a fluid-phase fluorescence marker, rhodamine dextran (0.5 mg/ml) (red), for a 3- to 4-h period, extensively washed, and then examined by confocal microscopy.

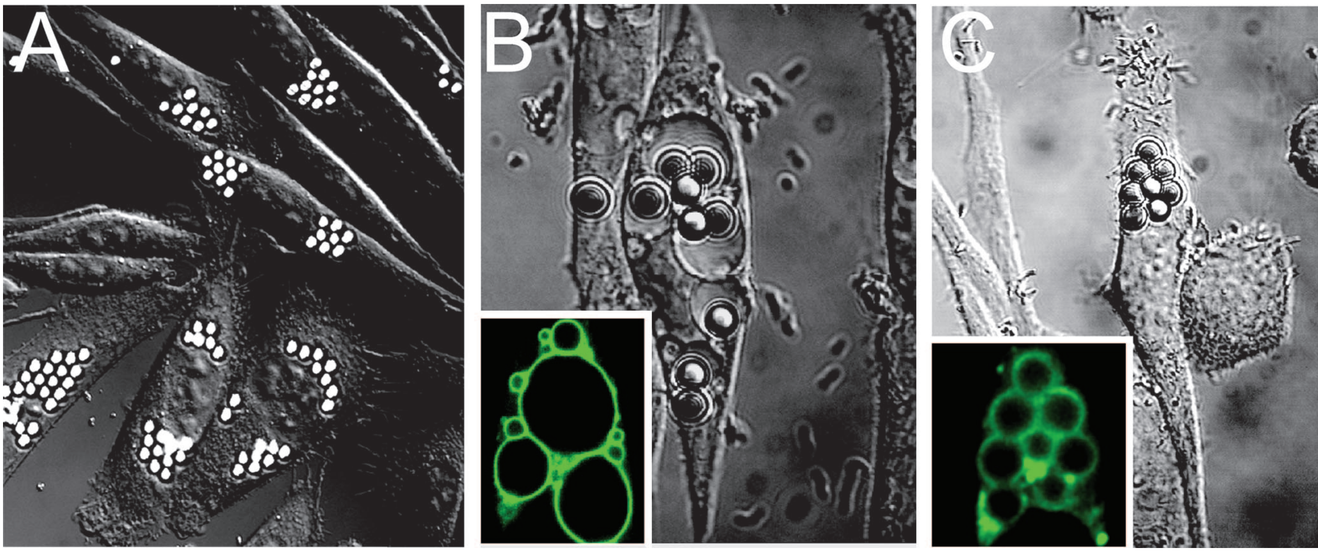

FIG. 6. *H. pylori* causes fusion of phagolysosome compartments in CHOIIa cells. Panel A shows a DIC micrograph of 3-μm latex bead-containing phagolysosomes in CHOIIa cells. The exposure of CHOIIa cells to wild-type but not *vacA* mutant *H. pylori* caused the fusion of latex bead-containing phagolysosomes. (B and C) DIC images of latex bead-containing phagolysosomes in CHOIIa cells expressing GFP-Rab7 (green label in left corner of the panels) invaded with wild-type (B) or *vacA* mutant (C) *H. pylori* strains.

the transport and fusion of late endosomal and lysosomal compartments (36). Similar to other small GTPases, Rab7 cycles between an inactive cytoplasmic GDP-bound conformation and an active GTP-bound membrane conformation (36). Previous studies assessing the effect of purified toxin in mammalian cells have shown that toxin-induced vacuolation can be prevented by expression of a dominant-negative GDP-restricted Rab7 isoform (21, 28). Therefore, we next studied how Rab7 participates in the development of the bacterial intracellular niche. The switch and interswitch regions are conserved domains in Rab proteins that play a fundamental role in the interaction of these small GTPases with their effectors or regulators (53). We utilized transient expression of GFP-Rab7 F45A, a lack-of-function Rab7 isoform mutated in the interswitch region that does not associate with endocytic compartments but remains soluble in the cytoplasm (53). GFP-Rab7 F45A was not recruited to the vacuolar membrane and did not interfere with the formation of the bacterial intracellular niche, indicating that Rab7 VacA-mediated recruitment requires a functional Rab7 molecule (Fig. 8A and B). To characterize the state of activation of Rab7 localized to the vacuolar membrane, we utilized RILP. Rab7-RILP interactions are required for the microtubule-mediated transport and fusion of late endosomal and lysosomal compartments (20). RILP binds only to Rab7 in its active GTP-bound state, facilitating the interaction of dynein-dynactin motor complexes with late endosomes and lysosomes (8). When AGS cells expressing a GFP-RILP fusion protein were infected with *H. pylori*, RILP was strongly recruited to the VacA-mediated bacterial vacuoles (Fig. 8C and see Fig. S4A in the supplemental material) indicating that Rab7 in the vacuolar membrane is in its active conformation. To confirm the state of activation of Rab7 recruited to the *H. pylori* vacuole, we utilized FRAP of GFP-Rab7 in AGS cells. Photobleaching recovery of membrane-bound Rab7 occurs when the small GTPase dissociates from the membrane and is replaced by cytoplasmic GFP-Rab7 (49). This technique has been successfully applied to identify alterations in the cycling of active Rab7 in vivo (49). A representative result from one FRAP experiment is illustrated in Fig. 9A. A comparison of fluorescence recovery kinetics obtained for bleached *H. pylori*-containing vacuoles and late endosomes in AGS cells showed a marked reduction of GFP-Rab7 fluorescence recovery (mobile fraction) from the bacterial compartment (96.4% ± 7.8% in control endosomes to 26.0% ± 3.7% in vacuoles from infected cells) (Fig. 9A and B). The poor recovery of GFP-Rab7 fluorescence indicates an interruption of its normal turnover and, hence, retention of the active small GTPase at the vacuolar compartment.

We next characterized the role of the Rab7-RILP interaction in the formation of the bacterial niche by utilizing mutated forms of Rab7 or RILP. RILP interacts with two different regions of GTP-bound Rab7, the switch and interswitch regions, as well as the hypervariable RabSF motifs, RabSF1 and RabSF4 (53). Replacement of Val180 with Ala in RabSF4 region of Rab7 (Rab7 V180A) dramatically reduces its interaction with RILP (53) without affecting its capacity to bind endosomal compartments (data not shown). As shown in Fig. 8, Rab7 V180A was recruited to small bacterium-containing compartments. However, Rab7 V180A expression in AGS cells efficiently abrogated the formation of the large VacA-mediated bacterial niche (Fig. 8D and H); indicating that the interaction between Rab7 and RILP is essential for the morphogenesis of this compartment.

The participation of RILP in the formation of the VacA-mediated bacterial compartment was further investigated utilizing mutated isoforms of this molecule. The binding of RILP to Rab7 occurs through a protein domain that forms a coiled-coil homodimer that interacts with two GTP Rab7 molecules forming a Rab7-(RILP)2-Rab7 complex (9, 53). The replacement of Ile 251 with Ala in RILP disrupts its Rab7 interacting

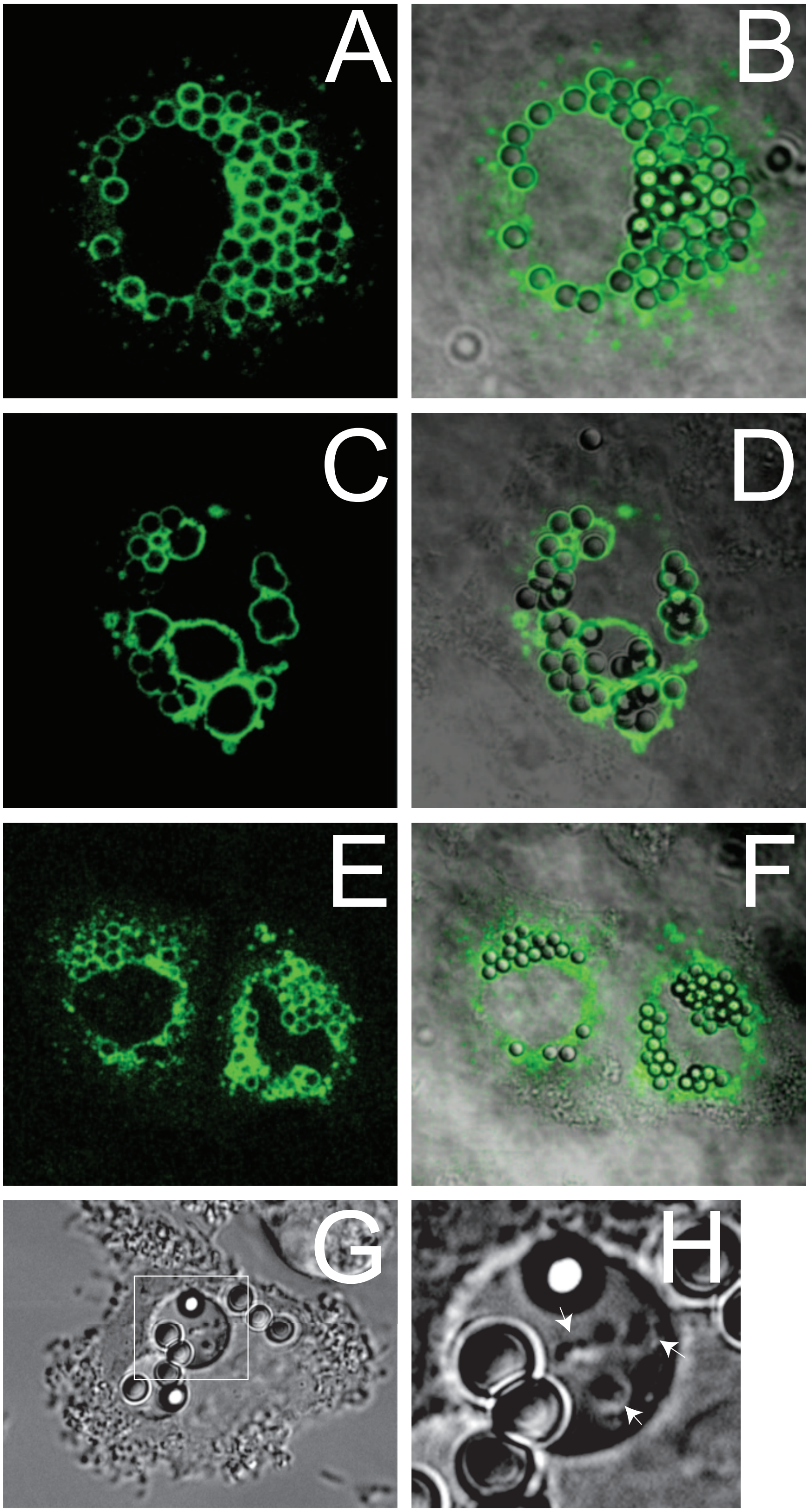

FIG. 7. *H. pylori* invasion causes fusion of phagolysosome and bacterial compartments in FcIIa-expressing AGS cells. Panel A shows a fluorescent confocal micrograph of GFP-Rab7-positive phagosomes in FcIIa-expressing AGS cells, and panel B shows the merged image with the bright-field micrograph showing single 3-μm latex beads contained in each of the compartments. The exposure of AGS cells to wild-type *H. pylori* for a 12-h period caused the fusion of latex bead-containing phagolysosomes to form large GFP-Rab7-positive vacuoles (C), which contain multiple latex beads as shown in panel D. The exposure of AGS cells to *vacA* mutant *H. pylori* for a 12-h period did not alter the morphology of Rab7-positive engineered phagolysosomes (E and F). A DIC micrograph of an AGS cell infected with *H. pylori* containing multiple 3-μm latex beads in single large vacuoles is shown in panel G. Panel H shows details of the vacuole indicated in panel G. The arrows in panel H show motile intracellular *H. pylori* cells sharing the same vacuolar compartment with latex beads.

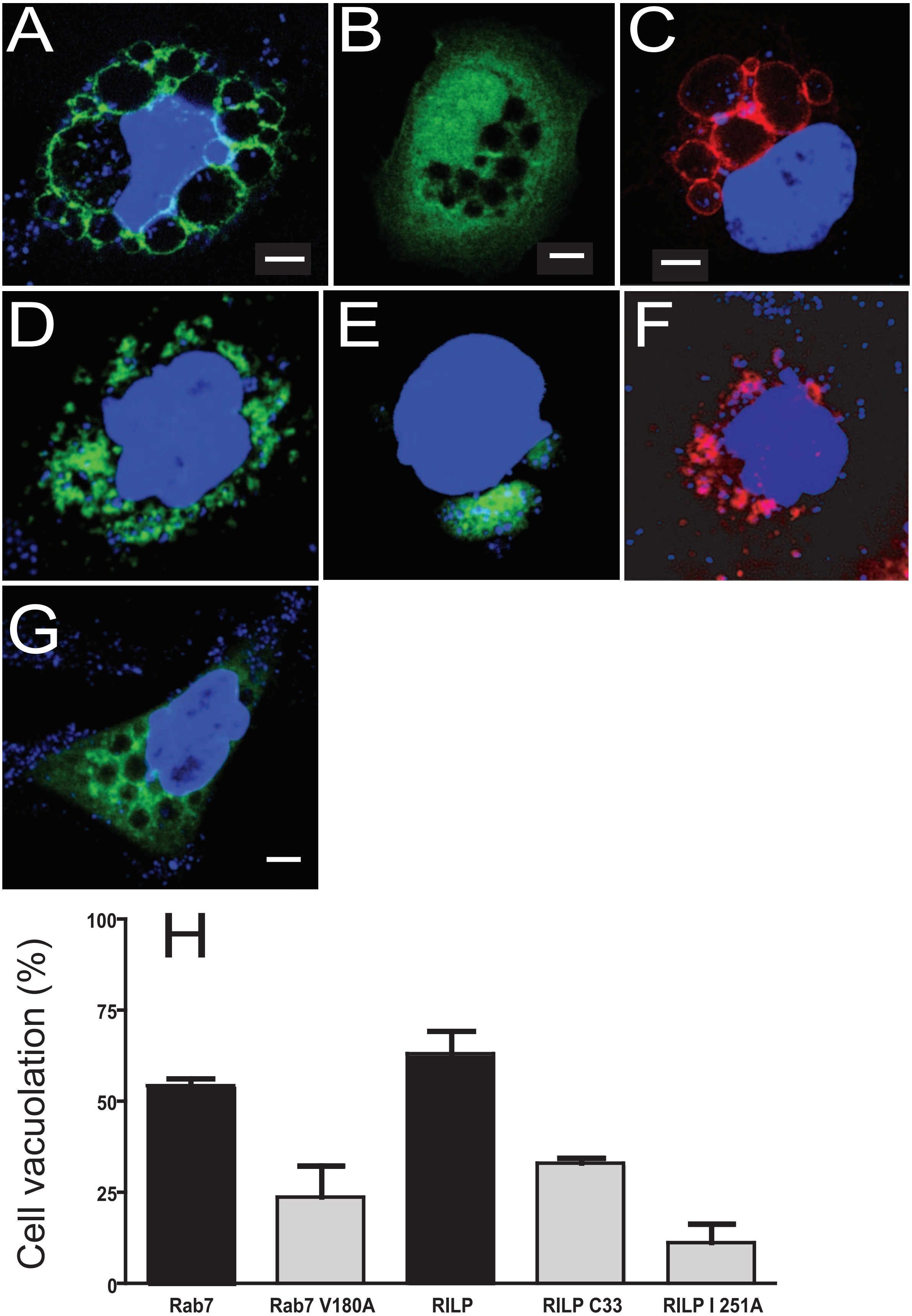
A
B
C
D
E
F
G
H
Cell vacuolation (%)
100
75
50
25
0
Rab7
Rab7 V180A
RILP
RILP C33
RILP I 251A

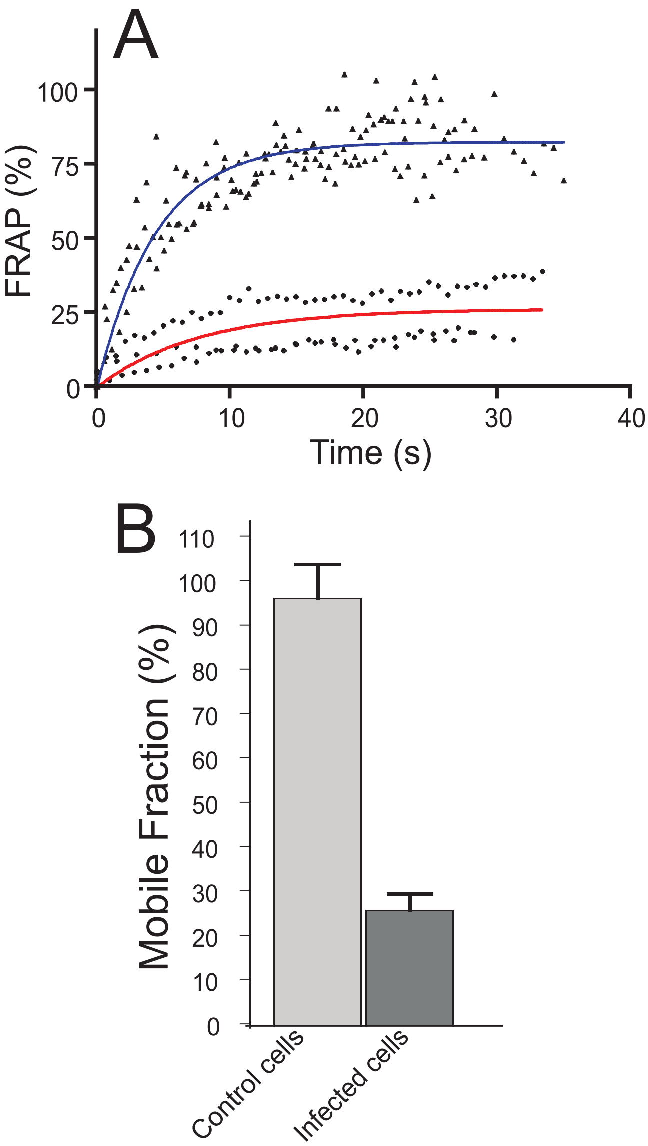

FIG. 9. VacA-positive *H. pylori* cells recruit and retain active Rab7 to their intracellular compartment. AGS cells were transfected with GFP-Rab7 and then infected with *H. pylori* for 24 h. GFP-Rab7 mobility was then estimated by FRAP. Panel A shows a representative quantitation and nonlinear regression fitted curve of the fluorescent recovery of Rab7 in endosomes from uninfected cells (blue line and triangles) and the *H. pylori* compartment (red line and squares). The summary of the fractional recovery of Rab7 in endosomes (light gray bar) and bacterial vacuoles (dark gray bar) from invaded cells is shown in panel B. Data are mean ± standard error of 10 cells.

domain so that the RILP I251A mutant does not bind to Rab7 (9, 53). Expression of RILP I251A in AGS cells caused a polarized distribution of Rab7 to areas adjacent to the nucleus (see Fig. S4 in the supplemental material) and disrupted the formation of the large VacA-mediated bacterial compartment in infected cells (Fig. 8E and H). RILPC33 is a truncated form of the protein lacking the N-terminal half, which cannot interact with microtubule motors but still binds to active Rab7, thereby blocking its interaction with the microtubule network and preventing fusion of late endosomes and/or lysosomes (8, 20). RILPC33-GFP efficiently abrogated the formation of large *H. pylori*-containing vacuoles, but not the recruitment of Rab7 to the bacterial compartment. (Fig. 8F to H and Fig. S4 in the supplemental material). In contrast, the small GTPase Rab34, which also participates in lysosome biogenesis and binds RILP in its active conformation (9, 50), did not localize to the large intracellular *H. pylori* compartment (Fig. 8G).

Taken together, the findings from (i) FRAP, (ii) RILP colocalization, and (iii) the use of RILP and Rab7 mutant isoforms suggest that VacA-positive *H. pylori* recruits and retains active Rab7 at the vacuolar membrane. In addition, a functional Rab7-RILP complex and interaction with the microtubule network are necessary for the formation of the bacterial compartment in AGS cells.

DISCUSSION

Many invasive pathogens have evolved strategies to protect their membrane-bound compartment by disrupting normal endosomal maturation and fusion with lysosomes, thereby promoting intracellular survival (45). The results presented here indicate that *H. pylori* utilizes a novel mechanism to evade lysosomal destruction in host cells.

Consistent with previous reports (3, 34), we found that *H. pylori* can invade and survive in AGS cells. These findings contrast with a previous report by Rittig and colleagues (39), who only rarely observed large vacuoles containing bacteria in AGS cells. A difference in experimental design likely explains the apparent discrepancy between our results and those of Rittig et al. (39). Similar to the findings of Ameiva et al. (3), we confirmed that the ability of *H. pylori* to invade AGS cells was independent of the vacuolating toxin VacA. In previous studies, Petersen et al. (35) demonstrated that VacA-positive bacteria had improved survival in epithelial cells up to 24 h but the mechanism responsible for the effect was not determined. In contrast, Amieva and colleagues (3) reported in their discussion that VacA did not alter intracellular survival in the time

FIG. 8. Rab7 and its effector RILP are necessary for the morphogenesis of *H. pylori*-containing vacuoles. Wild-type GFP-Rab7 (green) (A), but not GFP-Rab7 mutant F45A (green) (B), was recruited to *H. pylori* (blue)-containing vacuoles in AGS cells following 24 h of invasion (A and B, respectively). The Rab7 effector protein GFP-RILP (red) was recruited to *H. pylori* (blue)-containing vacuoles in AGS cells after 24 h of infection (C). Panel D shows that the expression of the GFP-Rab7 mutant, V180A (green), in AGS cells inhibited the formation of the large intracellular bacterial compartment after 24 h of infection. Panel E depicts inhibition of the large bacterium-containing compartment when the myc-tagged RILP mutant I251A is coexpressed with GFP-Rab7 (green) in AGS cells. Coexpression of myc-tagged Rab7 and mutant RILP C33 GFP (red) inhibits the morphogenesis of *H. pylori*'s (blue) large compartment (F) at 24 h of infection. Panel G shows the distribution of Rab34 GFP (green) in AGS cells after 24 h of infection with *H. pylori* (blue). Panel H shows quantitation of bacterium-mediated vacuolation in *H. pylori*-infected cells transfected with various mutant forms of Rab7 or RILP. One hundred cells in three independent experiments were scored for vacuole formation 24 h after bacterial invasion. Data are mean ± standard error. *H. pylori* cells were stained with the nucleic acid dye DAPI (4′,6′-diamidino-2-phenylindole) (blue).

frame assessed in their specific studies. However, the authors did suggest that further studies may identify an effect mediated by the toxin. Indeed, our findings clearly show a unique role for VacA as the main architect of the large bacterial intracellular niche, which mediates enhanced long-term survival of the bacteria.

Our studies indicate that the wild-type bacterial compartment originates from fusion of late endosomal and lysosomal compartments since characteristic markers of these compartments were present on bacterium-containing vacuoles. In addition, the pH of the bacterium-containing vacuoles was comparable to that of late endosomes. However, unlike the tight compartments containing VacA-negative bacteria, the large VacA-dependent bacterial vacuoles were devoid of the lysosomal protease cathepsin D. Furthermore, these compartments were unable to degrade endocytosed cargo. Taken together, our findings indicate that wild-type bacteria disrupt vacuole maturation at a late stage, preventing destruction by lysosomal proteases.

Small Rab GTPases associate with specific organelles, where they play a central role in targeting and recruiting a variety of effector proteins involved in directing membrane traffic. Since small GTPases play a fundamental role in the modulation of many cellular pathways, they are the preferential targets of several pathogens (5). Indeed, *Salmonella* recruits Rab7 to generate its intracellular compartment (19). Previous studies assessing the effect of purified VacA toxin alone in mammalian cells have shown that toxin-induced vacuolation can be prevented by GDP-restricted Rab7 isoform and, more recently, by the Rab7 binding protein oxysterol-binding protein, ORP1L (21, 28). However, since VacA has numerous effects on the host cell, whether or not the VacA-mediated enhanced intracellular survival was related to effects on Rab7 were unknown. Results from both FRAP experiments and transient expression of the downstream effector RILP indicate that VacA-positive bacteria efficiently hijack active Rab7 to the vacuolar compartment. In addition, retention of active Rab7 promoted fusion of late endosomal compartments, as demonstrated by fusion of vacuoles containing latex beads in engineered phagocytes. To our knowledge, the alteration of Rab7 function identified in the present study is a unique strategy exclusively employed by *H. pylori*. In contrast with *Salmonella*, which prevents the association of Rab7 with the downstream effector RILP (19), our studies clearly show that the interaction of Rab7, RILP, and the microtubule network was critical for the formation of the protected bacterial niche of VacA-positive *H. pylori*.

The mechanism(s) by which VacA-positive *H. pylori* hijacks Rab7 remains unknown. Current knowledge indicates that recruitment of Rab GTPases is mediated by proteins which regulate their GTP/GDP-bound state (reviewed in reference 36). Inactive GDP-bound Rabs are maintained in the cytoplasm in a complex with GDP displacement inhibitors (GDIs). Guanosine displacement factors displace Rabs from their complex with GDIs in the cytoplasm, allowing targeting to the membrane. Guanosine exchange factors then replace GDP by GTP, resulting in activation. GTPase-activating proteins can then hydrolyze GTP, allowing GDIs to remove the inactive Rab from the membrane. Currently, limited information exists with respect to the mammalian proteins which may regulate the GDP/GTP-bound state of Rab7 (38, 56). Based on the results of the FRAP experiments, which show a delay of Rab7 recovery during *H. pylori* infection, we hypothesize that interference with a GTPase-activating protein could provide an explanation for the VacA-mediated stabilization of the protein in its active conformation. Studies utilizing VacA-positive *H. pylori* should help to identify the factors which regulate Rab7 and delineate the mechanism responsible for Rab7 recruitment during infection.

A previous study indicates that treatment of mammalian cells with purified VacA toxin impairs the activation and sorting of cathepsin D, as well as the lysosomal degradation of epidermal growth factor (40). However, in the study by Satin and colleagues (40), an alteration in the pH of the lumen of endosomes and lysosomes of VacA-treated cells was detected and considered by the authors to account for the mistargeting. In our study, we demonstrated that the large bacterium-containing vacuoles lacked detectable cathepsin D and were impaired in their ability to degrade cargo. However, the pH of the large bacterium-containing vacuole was acidic; thus, an alteration in lysosomal pH would not explain the disruption of the endocytic pathway. Instead, we propose that the retention of active Rab7 by the VacA-positive bacterium-containing compartment alters endocytic trafficking, preventing endosomal maturation (18). Therefore, bacterial compartments in which active Rab7 is retained would utilize harmless late endosomal-lysosomal compartments as a source of membrane to sustain its growth and generate a protective intracellular niche for *H. pylori*. Further studies will be required to define the exact mechanisms involved in this process. Disruption of the endocytic pathway could have several additional effects on host cells. For example, the previously described impairment of antigen degradation and presentation in VacA-intoxicated B lymphocytes could be due to disruption of the endocytic pathway (25).

In summary, we provide new evidence that supports a preponderant role for the VacA toxin in the generation and maintenance of an intracellular reservoir for the pathogen. In addition, we identify a unique mechanism by which *H. pylori* generates this niche which may contribute to the persistence of infection.

ACKNOWLEDGMENTS

We are grateful to Sergio Grinstein, John Brumell, and Philip Sherman from The Hospital for Sick Children, Toronto, Ontario, Canada, and Paul Saftig and Eeva Lisa Eskelinen for helpful discussion and critical reading of the manuscript.

M.T. is supported by Canadian Association of Gastroenterology/CIHR/AstraZeneca Canada, Inc., Fellowship Award. C.V. was supported by an ASM international studentship. N.L.J. is supported by a CIHR operating grant. S.R.B. is supported by NIH grant R01 AI45928.

REFERENCES

1. **Alonso, A., and F. Garcia-del Portillo.** 2004. Hijacking of eukaryotic functions by intracellular bacterial pathogens. Int. Microbiol. **7:**181–191.
2. **Amano, T., T. Furuno, N. Hirashima, N. Ohyama, and M. Nakanishi.** 2001. Dynamics of intracellular granules with CD63-GFP in rat basophilic leukemia cells. J. Biochem. (Tokyo) **129:**739–744.
3. **Amieva, M. R., N. R. Salama, L. S. Tompkins, and S. Falkow.** 2002. Helicobacter pylori enter and survive within multivesicular vacuoles of epithelial cells. Cell Microbiol. **4:**677–690.
4. **Boncristiano, M., S. R. Paccani, S. Barone, C. Ulivieri, L. Patrussi, D. Ilver, A. Amedei, M. M. D'Elios, J. L. Telford, and C. T. Baldari**. 2003. The Helicobacter pylori vacuolating toxin inhibits T cell activation by two independent mechanisms. J. Exp. Med. **198:**1887–1897.

5. **Boquet, P., and E. Lemichez.** 2003. Bacterial virulence factors targeting Rho GTPases: parasitism or symbiosis? Trends Cell Biol. **13:**238–246.
6. **Botelho, R. J., D. J. Hackam, A. D. Schreiber, and S. Grinstein.** 2000. Role of COPI in phagosome maturation. J. Biol. Chem. **275:**15717–15727.
7. **Brumell, J. H., and S. Grinstein.** 2004. Salmonella redirects phagosomal maturation. Curr. Opin. Microbiol. **7:**78–84.
8. **Cantalupo, G., P. Alifano, V. Roberti, C. B. Bruni, and C. Bucci.** 2001. Rab-interacting lysosomal protein (RILP): the Rab7 effector required for transport to lysosomes. EMBO J. **20:**683–693.
9. **Colucci, A. M., M. C. Campana, M. Bellopede, and C. Bucci.** 2005. The Rab-interacting lysosomal protein, a Rab7 and Rab34 effector, is capable of self-interaction. Biochem. Biophys. Res. Commun. **334:**128–133.
10. **Cover, T. L., and S. R. Blanke.** 2005. Helicobacter pylori VacA, a paradigm for toxin multifunctionality. Nat. Rev. Microbiol. **3:**320–332.
11. **Cover, T. L., U. S. Krishna, D. A. Israel, and R. M. Peek, Jr.** 2003. Induction of gastric epithelial cell apoptosis by Helicobacter pylori vacuolating cytotoxin. Cancer Res. **63:**951–957.
12. **Cover, T. L., L. Y. Reddy, and M. J. Blaser.** 1993. Effects of ATPase inhibitors on the response of HeLa cells to *Helicobacter pylori* vacuolating toxin. Infect. Immun. **61:**1427–1431.
13. **Downey, G. P., R. J. Botelho, J. R. Butler, Y. Moltyaner, P. Chien, A. D. Schreiber, and S. Grinstein.** 1999. Phagosomal maturation, acidification, and inhibition of bacterial growth in nonphagocytic cells transfected with FcgammaRIIA receptors. J. Biol. Chem. **274:**28436–28444.
14. **Dubois, A.** 1995. Spiral bacteria in the human stomach: the gastric helicobacters. Emerg. Infect. Dis. **1:**79–85.
15. **Fischer, W., B. Gebert, and R. Haas.** 2004. Novel activities of the Helicobacter pylori vacuolating cytotoxin: from epithelial cells towards the immune system. Int. J. Med. Microbiol. **293:**539–547.
16. **Galmiche, A., J. Rassow, A. Doye, S. Cagnol, J. C. Chambard, S. Contamin, V. de Thillot, I. Just, V. Ricci, E. Solcia, E. Van Obberghen, and P. Boquet.** 2000. The N-terminal 34 kDa fragment of Helicobacter pylori vacuolating cytotoxin targets mitochondria and induces cytochrome c release. EMBO J. **19:**6361–6370.
17. **Gebert, B., W. Fischer, and R. Haas.** 2004. The Helicobacter pylori vacuolating cytotoxin: from cellular vacuolation to immunosuppressive activities. Rev. Physiol. Biochem. Pharmacol. **152:**205–220.
18. **Ghosh, P., N. M. Dahms, and S. Kornfeld.** 2003. Mannose 6-phosphate receptors: new twists in the tale. Nat. Rev. Mol. Cell Biol. **4:**202–212.
19. **Harrison, R. E., J. H. Brumell, A. Khandani, C. Bucci, C. C. Scott, X. Jiang, B. B. Finlay, and S. Grinstein.** 2004. Salmonella impairs RILP recruitment to Rab7 during maturation of invasion vacuoles. Mol. Biol. Cell **15:**3146–3154.
20. **Harrison, R. E., C. Bucci, O. V. Vieira, T. A. Schroer, and S. Grinstein.** 2003. Phagosomes fuse with late endosomes and/or lysosomes by extension of membrane protrusions along microtubules: role of Rab7 and RILP. Mol. Cell. Biol. **23:**6494–6506.
21. **Johansson, M., M. Lehto, K. Tanhuanpaa, T. L. Cover, and V. M. Olkkonen.** 2005. The oxysterol-binding protein homologue ORP1L interacts with Rab7 and alters functional properties of late endocytic compartments. Mol. Biol. Cell **16:**5480–5492.
22. **Kanai, F., H. Liu, S. J. Field, H. Akbary, T. Matsuo, G. E. Brown, L. C. Cantley, and M. B. Yaffe.** 2001. The PX domains of p47phox and p40phox bind to lipid products of PI(3)K. Nat. Cell Biol. **3:**675–678.
23. **Kwok, T., S. Backert, H. Schwarz, J. Berger, and T. F. Meyer.** 2002. Specific entry of *Helicobacter pylori* into cultured gastric epithelial cells via a zipper-like mechanism. Infect. Immun. **70:**2108–2120.
24. **Li, Y., A. Wandinger-Ness, J. R. Goldenring, and T. L. Cover.** 2004. Clustering and redistribution of late endocytic compartments in response to Helicobacter pylori vacuolating toxin. Mol. Biol. Cell **15:**1946–1959.
25. **Molinari, M., M. Salio, C. Galli, N. Norais, R. Rappuoli, A. Lanzavecchia, and C. Montecucco.** 1998. Selective inhibition of Ii-dependent antigen presentation by Helicobacter pylori toxin VacA. J. Exp. Med. **187:**135–140.
26. **Nguyen, V. Q., R. M. Caprioli, and T. L. Cover.** 2001. Carboxy-terminal proteolytic processing of *Helicobacter pylori* vacuolating toxin. Infect. Immun. **69:**543–546.
27. **Oh, J. D., S. M. Karam, and J. I. Gordon.** 2005. Intracellular Helicobacter pylori in gastric epithelial progenitors. Proc. Natl. Acad. Sci. USA **102:**5186–5191.
28. **Papini, E., B. Satin, C. Bucci, M. de Bernard, J. L. Telford, R. Manetti, R. Rappuoli, M. Zerial, and C. Montecucco.** 1997. The small GTP binding protein rab7 is essential for cellular vacuolation induced by Helicobacter pylori cytotoxin. EMBO J. **16:**15–24.
29. **Papini, E., B. Satin, N. Norais, M. de Bernard, J. L. Telford, R. Rappuoli, and C. Montecucco.** 1998. Selective increase of the permeability of polarized epithelial cell monolayers by Helicobacter pylori vacuolating toxin. J. Clin. Investig. **102:**813–820.
30. **Patel, H. K., D. C. Willhite, R. M. Patel, D. Ye, C. L. Williams, E. M. Torres, K. B. Marty, R. A. MacDonald, and S. R. Blanke.** 2002. Plasma membrane cholesterol modulates cellular vacuolation induced by the *Helicobacter pylori* vacuolating cytotoxin. Infect. Immun. **70:**4112–4123.
31. **Peek, R. M., Jr., and M. J. Blaser.** 2002. Helicobacter pylori and gastrointestinal tract adenocarcinomas. Nat. Rev. Cancer **2:**28–37.
32. **Perret, E., A. Lakkaraju, S. Deborde, R. Schreiner, and E. Rodriguez-Boulan.** 2005. Evolving endosomes: how many varieties and why? Curr. Opin. Cell Biol. **17:**423–434.
33. **Petersen, A. M., J. Blom, L. P. Andersen, and K. A. Krogfelt.** 2000. Role of strain type, AGS cells and fetal calf serum in Helicobacter pylori adhesion and invasion assays. FEMS Immunol. Med. Microbiol. **29:**59–67.
34. **Petersen, A. M., and K. A. Krogfelt.** 2003. Helicobacter pylori: an invading microorganism? A review. FEMS Immunol. Med. Microbiol. **36:**117–126.
35. **Petersen, A. M., K. Sorensen, J. Blom, and K. A. Krogfelt.** 2001. Reduced intracellular survival of Helicobacter pylori vacA mutants in comparison with their wild-types indicates the role of VacA in pathogenesis. FEMS Immunol. Med. Microbiol. **30:**103–108.
36. **Pfeffer, S., and D. Aivazian.** 2004. Targeting Rab GTPases to distinct membrane compartments. Nat. Rev. Mol. Cell. Biol. **5:**886–896.
37. **Rieder, G., W. Fischer, and R. Haas.** 2005. Interaction of Helicobacter pylori with host cells: function of secreted and translocated molecules. Curr. Opin. Microbiol. **8:**67–73.
38. **Rink, J., E. Ghigo, Y. Kalaidzidis, and M. Zerial.** 2005. Rab conversion as a mechanism of progression from early to late endosomes. Cell **122:**735–749.
39. **Rittig, M. G., B. Shaw, D. P. Letley, R. J. Thomas, R. H. Argent, and J. C. Atherton.** 2003. Helicobacter pylori-induced homotypic phagosome fusion in human monocytes is independent of the bacterial vacA and cag status. Cell Microbiol. **5:**887–899.
40. **Satin, B., N. Norais, J. Telford, R. Rappuoli, M. Murgia, C. Montecucco, and E. Papini.** 1997. Effect of Helicobacter pylori vacuolating toxin on maturation and extracellular release of procathepsin D and on epidermal growth factor degradation. J. Biol. Chem. **272:**25022–25028.
41. **Suerbaum, S., and P. Michetti.** 2002. Helicobacter pylori infection. N. Engl. J. Med. **347:**1175–1186.
42. **Sundrud, M. S., V. J. Torres, D. Unutmaz, and T. L. Cover.** 2004. Inhibition of primary human T cell proliferation by Helicobacter pylori vacuolating toxin (VacA) is independent of VacA effects on IL-2 secretion. Proc. Natl. Acad. Sci. USA **101:**7727–7732.
43. **Suzuki, J., H. Ohnishi, A. Wada, T. Hirayama, H. Ohno, N. Ueda, H. Yasuda, T. Iiri, Y. Wada, M. Futai, and H. Mashima.** 2003. Involvement of syntaxin 7 in human gastric epithelial cell vacuolation induced by the Helicobacter pylori-produced cytotoxin VacA. J. Biol. Chem. **278:**25585–25590.
44. **Suzuki, J., H. Ohnsihi, H. Shibata, A. Wada, T. Hirayama, T. Iiri, N. Ueda, C. Kanamaru, T. Tsuchida, H. Mashima, H. Yasuda, and T. Fujita.** 2001. Dynamin is involved in human epithelial cell vacuolation caused by the Helicobacter pylori-produced cytotoxin VacA. J. Clin. Investig. **107:**363–370.
45. **Swanson, M. S., and E. Fernandez-Moreira.** 2002. A microbial strategy to multiply in macrophages: the pregnant pause. Traffic **3:**170–177.
46. **Szabo, I., S. Brutsche, F. Tombola, M. Moschioni, B. Satin, J. L. Telford, R. Rappuoli, C. Montecucco, E. Papini, and M. Zoratti.** 1999. Formation of anion-selective channels in the cell plasma membrane by the toxin VacA of Helicobacter pylori is required for its biological activity. EMBO J. **18:**5517–5527.
47. **Telford, J. L., P. Ghiara, M. Dell'Orco, M. Comanducci, D. Burroni, M. Bugnoli, M. F. Tecce, S. Censini, A. Covacci, Z. Xiang, et al.** 1994. Gene structure of the Helicobacter pylori cytotoxin and evidence of its key role in gastric disease. J. Exp. Med. **179:**1653–1658.
48. **Torres, V. J., M. S. McClain, and T. L. Cover.** 2004. Interactions between p-33 and p-55 domains of the Helicobacter pylori vacuolating cytotoxin (VacA). J. Biol. Chem. **279:**2324–2331.
49. **Vieira, O. V., C. Bucci, R. E. Harrison, W. S. Trimble, L. Lanzetti, J. Gruenberg, A. D. Schreiber, P. D. Stahl, and S. Grinstein.** 2003. Modulation of Rab5 and Rab7 recruitment to phagosomes by phosphatidylinositol 3-kinase. Mol. Cell. Biol. **23:**2501–2514.
50. **Wang, T., and W. Hong.** 2002. Interorganellar regulation of lysosome positioning by the Golgi apparatus through Rab34 interaction with Rab-interacting lysosomal protein. Mol. Biol. Cell **13:**4317–4332.
51. **Willhite, D. C., T. L. Cover, and S. R. Blanke.** 2003. Cellular vacuolation and mitochondrial cytochrome c release are independent outcomes of Helicobacter pylori vacuolating cytotoxin activity that are each dependent on membrane channel formation. J. Biol. Chem. **278:**48204–48209.
52. **Willhite, D. C., D. Ye, and S. R. Blanke.** 2002. Fluorescence resonance energy transfer microscopy of the *Helicobacter pylori* vacuolating cytotoxin within mammalian cells. Infect. Immun. **70:**3824–3832.
53. **Wu, M., T. Wang, E. Loh, W. Hong, and H. Song.** 2005. Structural basis for recruitment of RILP by small GTPase Rab7. EMBO J. **24:**1491–1501.
54. **Wyle, F. A., A. Tarnawski, D. Schulman, and W. Dabros.** 1990. Evidence for

gastric mucosal cell invasion by C. pylori: an ultrastructural study. J. Clin. Gastroenterol. **12**(Suppl. 1)**:**S92–S98.
55. **Ye, D., and S. R. Blanke.** 2002. Functional complementation reveals the importance of intermolecular monomer interactions for Helicobacter pylori VacA vacuolating activity. Mol. Microbiol. **43:**1243–1253.
56. **Zhang, X. M., B. Walsh, C. A. Mitchell, and T. Rowe.** 2005. TBC domain family, member 15 is a novel mammalian Rab GTPase-activating protein with substrate preference for Rab7. Biochem. Biophys. Res. Commun. **335:** 154–161.
57. **Zheng, P. Y., and N. L. Jones.** 2003. Helicobacter pylori strains expressing the vacuolating cytotoxin interrupt phagosome maturation in macrophages by recruiting and retaining TACO (coronin 1) protein. Cell Microbiol. **5:**25–40.

Editor: D. L. Burns